We are IntechOpen, the world's leading publisher of Open Access books Built by scientists, for scientists

6,900
Open access books available

186,000
International authors and editors

200M
Downloads

Our authors are among the

154
Countries delivered to

TOP 1%
most cited scientists

12.2%
Contributors from top 500 universities

WEB OF SCIENCE™

Selection of our books indexed in the Book Citation Index in Web of Science™ Core Collection (BKCI)

Interested in publishing with us?
Contact book.department@intechopen.com

Numbers displayed above are based on latest data collected.
For more information visit www.intechopen.com

High-Speed Railway Tunnel Hood: Seismic Dynamic Characteristic Analysis

Wang Ying-xue, He Jun, Jian Ming,
Chang Qiao-lei and Ren Wen-qiang

Additional information is available at the end of the chapter

http://dx.doi.org/10.5772/66811

Abstract

When a high-speed train is passing through a tunnel, micro-compression wave may be created at the tunnel exit, which will affect the environment around the railway line. Setting hood at tunnel entrance is one of the efficacious ways for solving this problem. While in an earthquake region, in addition to consideration of controlling micro-compression wave, the seismic safety of hood structure must not overlook the factor. In this chapter, using finite difference method, several types of hood seismic dynamic characteristic were analyzed, and their seismic dynamic respond stress curves were drawn out. As a result, the recommended hood type was determined, which is helpful for hood design in high intensity earthquake zone.

Keywords: tunnel, hood, seismic dynamic characteristic, finite difference method

1. Introduction

In China, high-speed railway technology got quick development and more and more high-speed railway tunnels were built in high earthquake intensity zones. Large amount of post-earthquake investigation shows that tunnel entrance is liable to earthquake effect and result in damage. However, for solving train-tunnel aerodynamic effect, tunnel hood has become an indispensable accessory of tunnel structure. So how to improve tunnel hood seismic characteristic is one of the hot point on tunnel seismic research.

To the tunnel entrance seismic character, much amount of research has been made and some important conclusions have been drawn out.

INTECH
open science | open minds

© 2017 The Author(s). Licensee InTech. This chapter is distributed under the terms of the Creative Commons Attribution License (http://creativecommons.org/licenses/by/3.0), which permits unrestricted use, distribution, and reproduction in any medium, provided the original work is properly cited. CC BY

Gao et al. (2009) did a thorough tunnel damage field investigation along the Dujiangyan-Wenchuan highway after the Wenchuan earthquake. The inspection results showed that the disaster induced relatively serious damage to the tunnel entrance.

Through collecting and analyzing information of seismic damage of the tunnel portals in Wenchuan earthquake, Wang et al. (2012) summed up the major factors that affected seismic damage extension, and pointed out using fuzzy synthetic evaluation method for the estimation of seismic risk level of mountain tunnel portals. Zheng (2007), using 3D distinct element method, analyzed the tunnel entrance seismic response. Cui (2010), using finite difference software FLAC-3D and experiment method, researched the seismic design calculation method of tunnel shallow-buried portal.

From previous discussion, it can be seen that many researchers have done study on tunnel entrance seismic character, while few topic pointed to the high-speed tunnel hood. In fact, for relief of aerodynamic effect, the hood structure usually set opening on top or side district. So in high seismic area, the tunnel hood will be more fragile compared with common tunnel portal.

In this chapter, using finite element software, Abaqus, the seismic character of two opening hood and nonopening hood was calculated and compared, and the recommended hood structure was given out. The types of hood are side-strip and top combination opening hood, two-side-strip opening hood and two seam opening hood.

2. Numerical simulation parameter

2.1. Numerical model

In this chapter, finite element software Abaqus was used for simulating the tunnel hood dynamic response under seismic wave. The dimension of the model is shown in **Table 1**.

Whole model	***x/m***	***y/m***	***z/m***	**Explanation**
	134.7	**100**	**77.8**	Yang slope degree is 45°, and vault buried depth is 30 m.
Tunnel hood	14.7	20	12.28	Cross-section area is 100 m^2; the thickness of the lining is 0.7 m.

Table 1. Model size and tunnel hood structure size.

For obtaining a good relief microcompression effect, the hood opening parameter must be determined through a large amount of analysis and calculation. Jiang (2014) gave out 20 m length of three types of hood optimum parameter, which is shown in **Figure 1**. The numerical model meshes of the whole model and hood structure are shown in **Figures 2** and **3**. For absorption of the seismic reflection wave, the cycle sides of the model is set as infinite element, and the bottom of the model is set as viscous-elastic boundary.

http://dx.doi.org/10.5772/66811

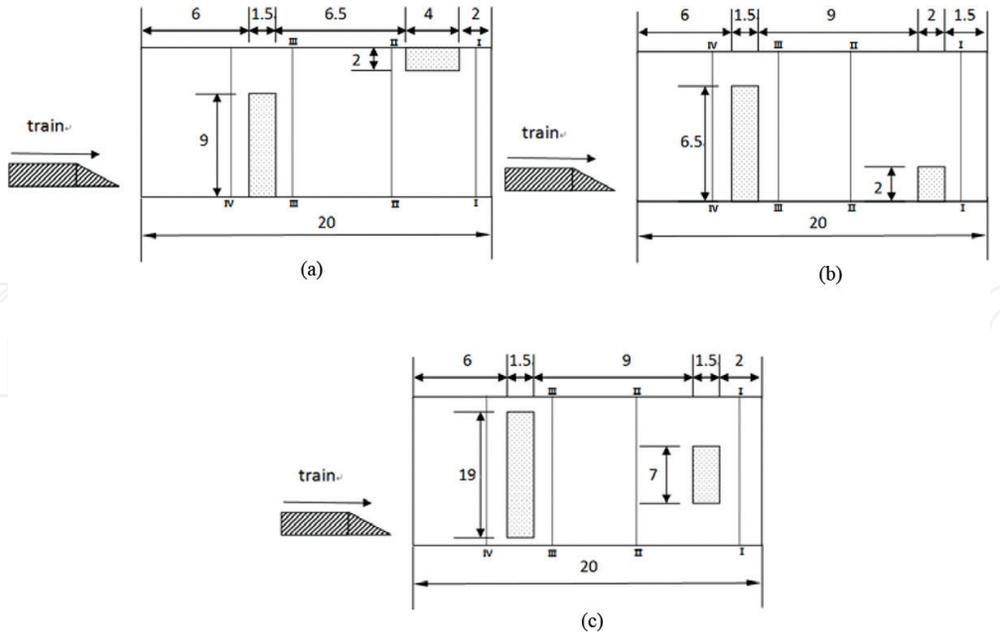

Figure 1. The diagram of the calculation model. (a) Side-strip and top combination opening hood (opening ratio = 45%). (b) Two-side-strip opening (opening ratio = 27.5%). (c) Two seam opening hood (opening ratio = 39%).

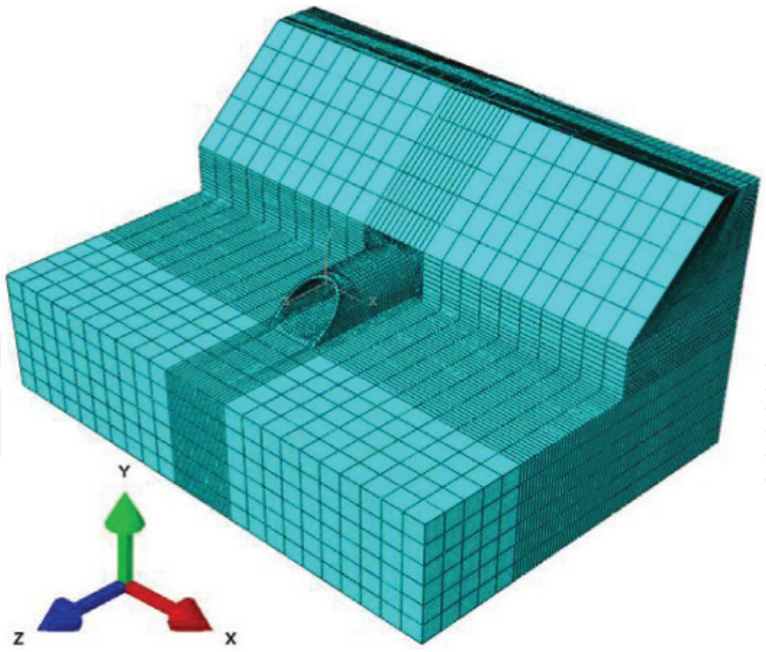

Figure 2. The arrangement plan of hood structure (units: m; bilateral symmetry).

The lining of the tunnel is C35 concrete and the surrounding rock is grade IV. Their mechanical parameters are shown in **Table 2**.

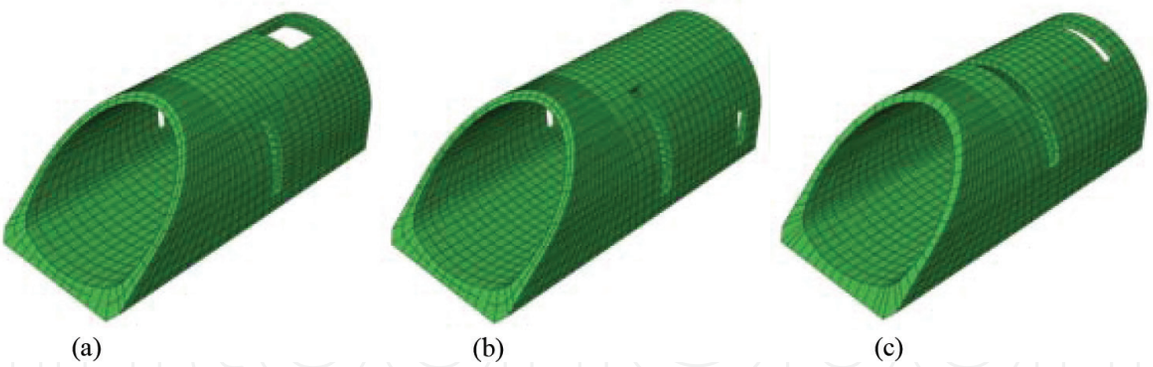

Figure 3. The model diagram of different hood structure. (a) Side-strip and top combination opening hood. (b) Two-side-strip opening hood. (c) Two seam opening hood.

Type of material	Density (kg/m^3)	Young modulus (GPa)	Poisson ratio	Cohesion force (MPa)	Friction angle (°)
Surrounding rock	2100	8	0.31	0.6	33
C35 concrete	2500	31.5	0.2	—	—

Table 2. Material mechanics parameters.

The input seismic wave is scaled Wolong wave and is shown in **Figure 4**, the acceleration pick of which was 0.62 m/s^2 and was set on the bottom of the model for simulating the seismic effect in vertical direction.

The calculation was divided into two steps. First, only setting gravity load, the initial stress condition of the whole model would be obtained. Second, using dynamic implicit model and setting seismic load at the bottom of the model, the dynamic response of the lining was simulated. In the tunnel cross-section, there are nine monitor points on the lining of the tunnel, as shown in **Figure 5**, for recording the dynamic response in different position. In the tunnel axis direction, the hood was set with four monitor in cross-section. The position to tunnel and hood crossing surface is 1 m (surface I-I), 7 m (surface II-II), 11.5 m (surface III-III), and 15 m (surface IV-IV), respectively, and is shown in **Figure 1**.

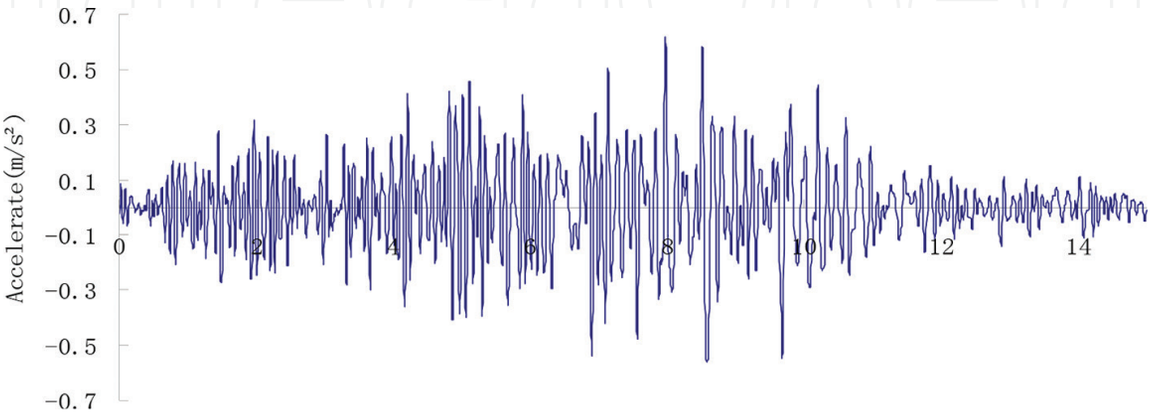

Figure 4. The accelerate curve of scaled Wolong wave.

http://dx.doi.org/10.5772/66811

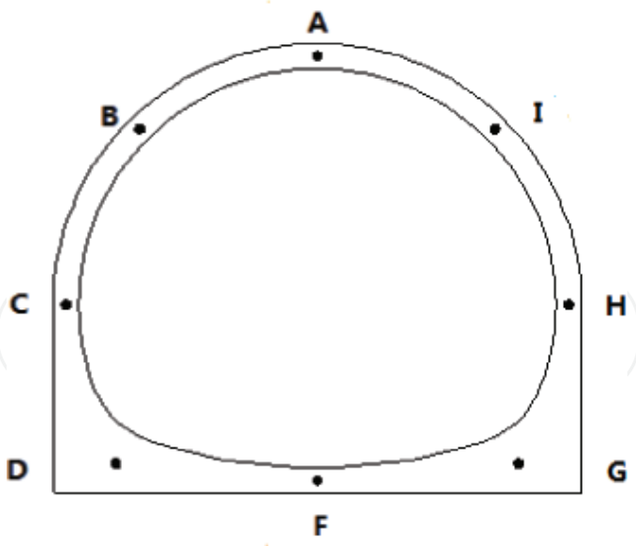

Figure 5. The schematic diagram of monitoring points.

3. Calculation result

3.1. Initial stress condition

Under dead weight of the surrounding rock and lining, the stress status of structure is almost the same to different calculation condition. So only the maximum principal stress contour graphic of side strip and top open combination opening hood was provided (**Figure 6**). It can be seen that the peak value of the maximum principal stress is 0.67 Mpa.

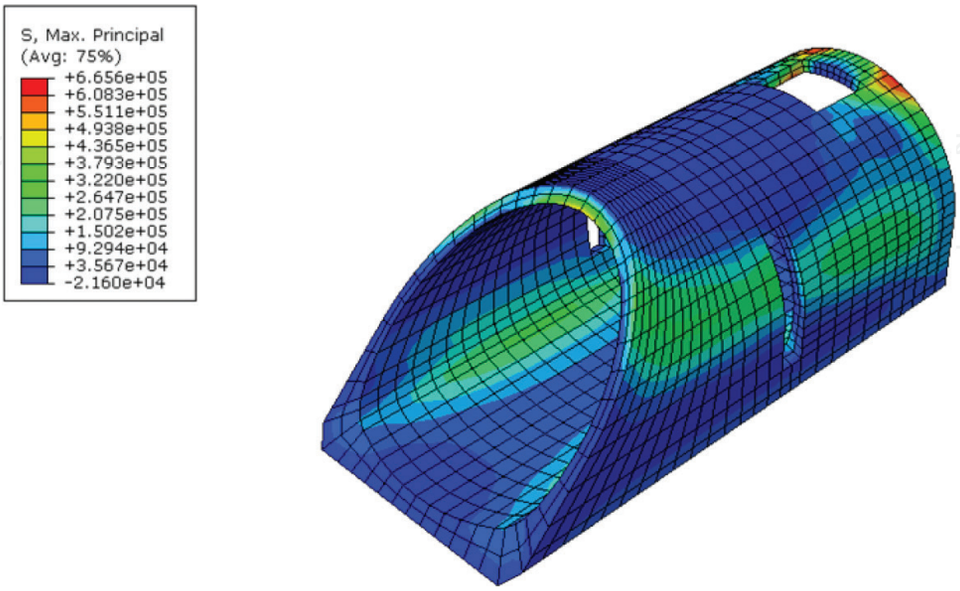

Figure 6. The max principal stress contour of side-strip and top combination opening hood structure.

3.2. Stress condition under seismic load

3.2.1. Stress contour condition analysis

The maximum principal stress conditions of the hood structures at peak period of seismic wave (t = 8.92) were shown in **Figure 7** and **Table 3**.

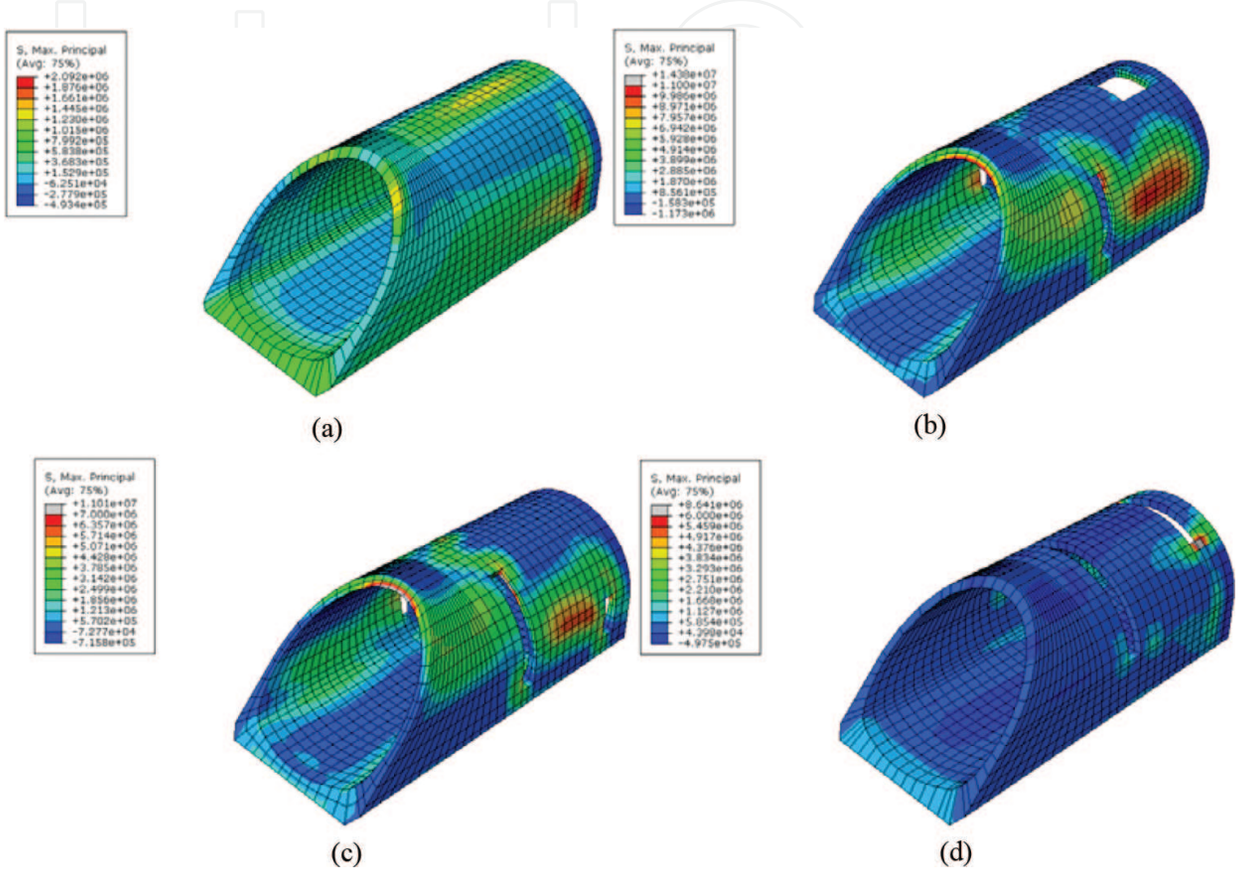

Figure 7. The max principal stress contour of different hood structure (T = 8.92 S). (a) No open. (b) Side-strip and top combination opening hood. (c) Two-side-strip opening hood. (d) Two seam opening hood.

Type of hood	No opening hood	Side-strip and top combination opening hood	Two-side-strip opening hood	Two seam opening hood
Value of maximum principal stress (MPa)	2.09	14.38	11.01	8.64

Table 3. The max principal stress of different hood structure.

The simulation results showed that:

1. Under seismic load, the peak value of maximum principal stress is more than 2 MPa. It can be checked out that the tensile strength of C35 is 1.57 MPa, which means that no matter of the setting opening, the seismic load can result in damage to the hood structure.

2. Differences of setting opening position can affect the peak value of maximum principal stress. Peak value of maximum principal stress to side-strip and top combination opening hood is up to 14.38 MPa, while the value to two seam opening hood is only 8.64 MPa. So choosing appropriate type of hood is very helpful for promoting structural safety in the earthquake region.

3.2.2. The stress condition discrepancy analysis

The discrepancy at hood cross-section and axial direction is shown in **Tables 4–7** and **Figures 8–11**.

Type of hood	Maximum principal stress/MPa							
	A	B	C	D	F	G	H	I
No open	0.87	-0.01	0.08	-0.11	0.01	-0.1	0.08	-0.01
Side-strip and top combination opening hood	2.17	0.02	2.93	1.82	0.02	1.81	2.82	0.03
Two-side-strip opening hood	0.01	0.05	2.89	-0.08	-0.03	-0.08	2.87	0.05
Two seam opening hood	0.11	2	0.04	-0.17	-0.002	-0.17	0.04	1.9

Table 4. The maximum principal stress of different hood structure at surface I-I.

Type of hood	Maximum principal stress/MPa							
	A	B	C	D	F	G	H	I
None opening hood	1.46	0.02	1.2	-0.06	0.1	-0.05	1.18	0.02
Side-strip and top combination opening hood	2.92	2.02	6.4	1.75	-0.01	1.75	6.43	2.02
Two-side-strip opening hood	0.98	0.71	4.1	1.26	-0.08	1.26	4.1	0.71
Two seam opening hood	-0.01	0.59	0.69	-0.04	0.12	-0.04	0.73	0.51

Table 5. The maximum principal stress of different hood structure at surface II-II.

Type of hood	Maximum principal stress/MPa							
	A	B	C	D	F	G	H	I
None opening hood	1.17	0.04	0.93	-0.07	0.11	-0.06	0.95	0.03
Side-strip and top combination opening hood	0.46	0.86	3.05	1.28	-0.01	1.27	3.06	0.83
Two-side-strip opening hood	0.05	0.13	1.18	0.85	0.01	0.85	1.18	0.12
Two seam opening hood	0.004	0.23	0.91	0.003	0.13	0.009	1.03	0.24

Table 6. The maximum principal stress of different hood structure at surface III-III.

Type of hood	Maximum principal stress/MPa							
	A	B	C	D	F	G	H	I
None opening hood	0.76	0.13	0.77	-0.08	0.12	-0.07	0.76	0.16
Side-strip and top combination opening hood	0.46	0.86	3.05	1.28	-0.01	1.27	3.06	0.83
Two-side-strip opening hood	2.08	1.5	3.2	0.58	-0.01	0.57	3.2	1.49
Two seam opening hood	0.06	0.12	1	0.05	0.13	0.05	1.16	0.12

Table 7. The max principal stress of different hood structure's surface IV-IV.

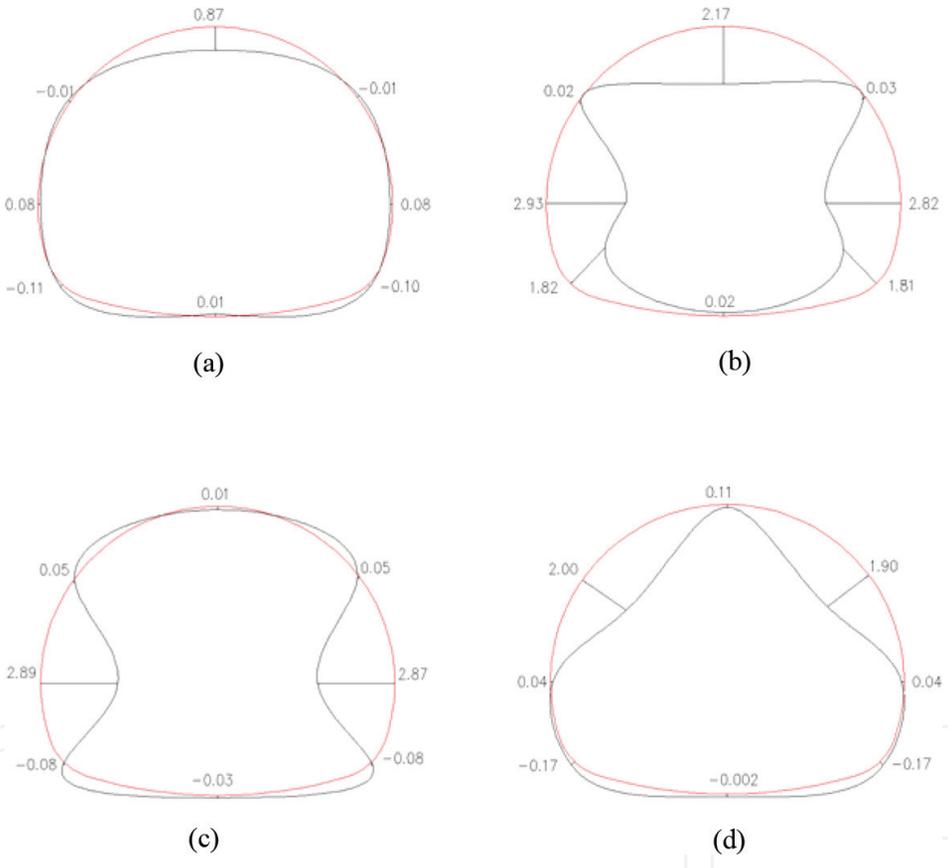

Figure 8. The max principal stress curve of different hood structure's surface I-I (units: Mpa). (a) None opening hood. (b) Side-strip and top combination opening hood. (c) Two-side-strip opening hood. (d) Two seam opening hood.

The results showed that:

1. Although there are some variations because of the differences in the type of hood, the stress maximum region is almost the same, near to the waist of the hood structure.
2. Except the two seam opening hood, in the hood axial direction, the peak value of max principal stress appeared at the section II-II, which is 7 m to the hood and tunnel cross point.

http://dx.doi.org/10.5772/66811

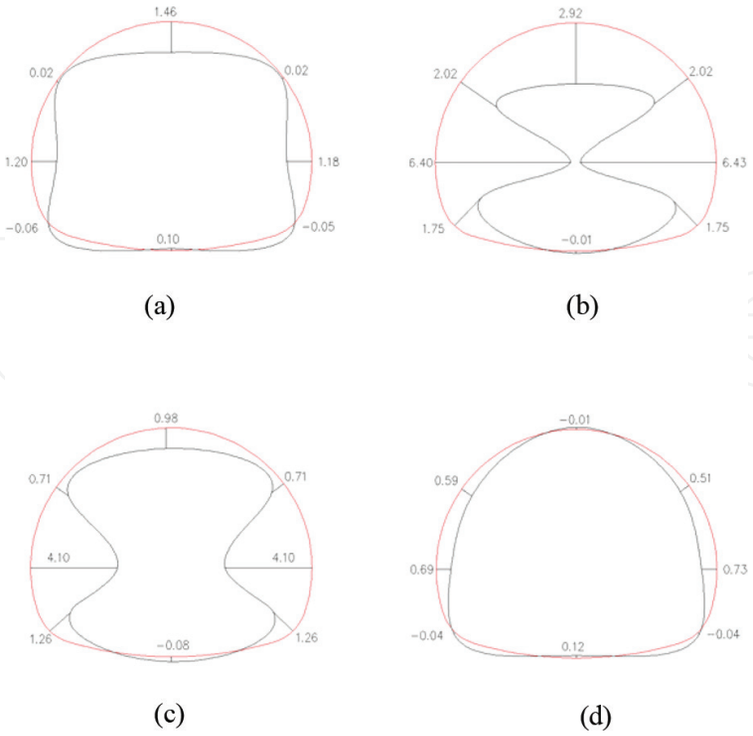

Figure 9. The max principal stress curve of different hood structure on surface II-II (units: Mpa). (a) None opening hood. (b) Side-strip and top combination opening hood. (c) Two-side-strip opening hood. (d) Two seam opening hood.

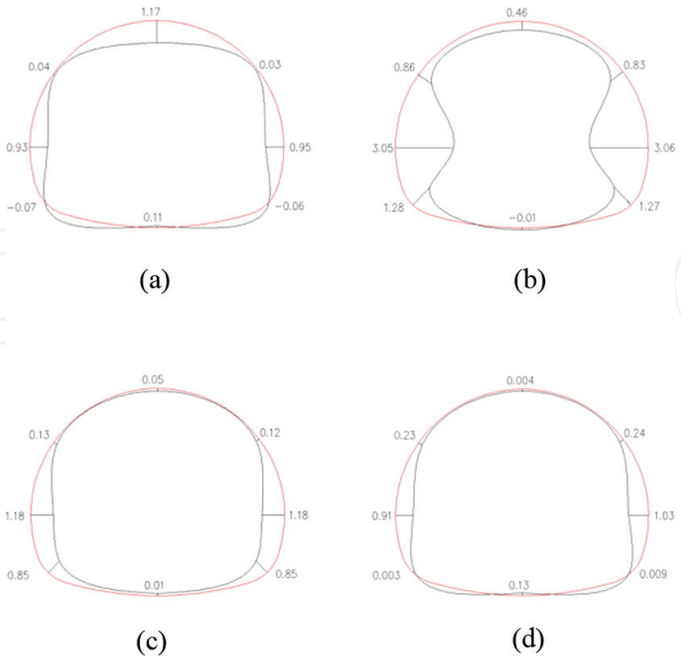

Figure 10. The max principal stress curve of different hood structure at surface III-III (units: Mpa). (a) None opening hood. (b) Side-strip and top combination opening hood. (c). Two-side-strip opening hood. (d) Two seam opening hood.

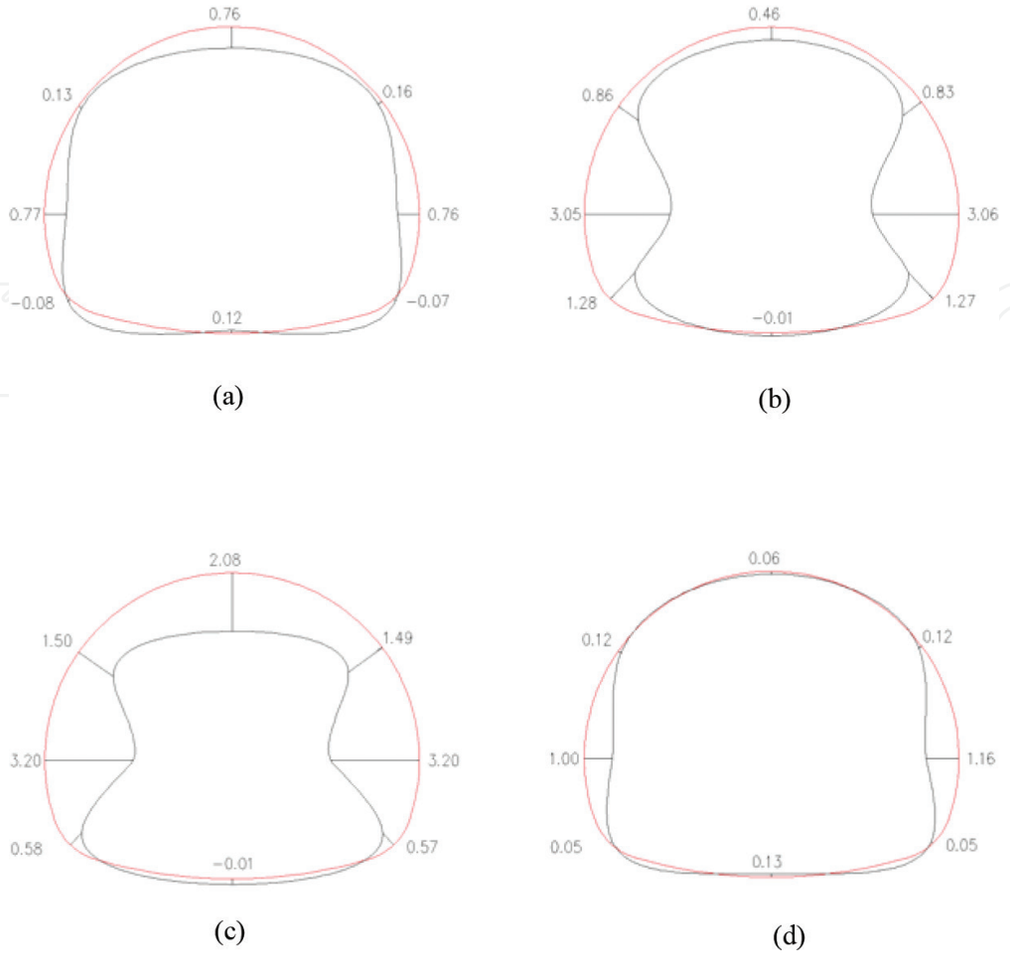

Figure 11. The max principal stress curve of different hood structure at surface IV-IV (units: Mpa). (a) No open. (b) Side-strip and top combination opening hood. (c) Two-side-strip opening hood. (d) Two seam opening hood.

3. Among these hoods, the peak value on two seam opening hood is the lowest. In some checking point, the max principal stress on its structure is even lower than that on no opening hood as shown in **Figure 12** and **Table 8**.

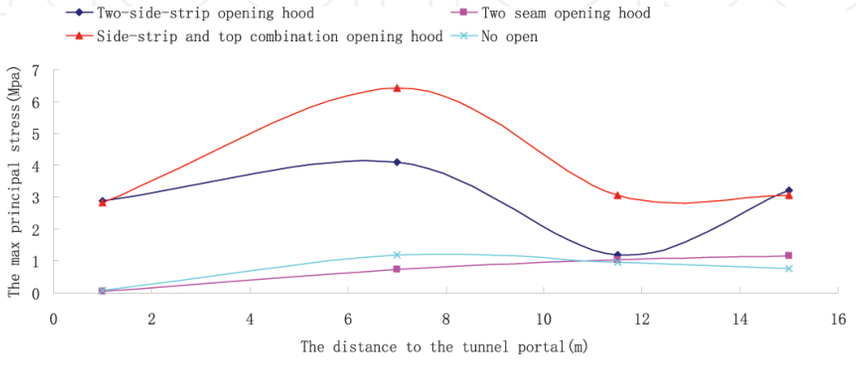

Figure 12. The max principal stress of different monitor cross-section at the waist of the hood structure.

Type of hood	Maximum principal stress value/Mpa			
	Section I-I	Section II-II	Section III-III	Section IV-IV
None opening hood	0.08	1.18	0.95	0.76
Side-strip and top combination opening hood	2.82	6.43	3.06	3.06
Two-side-strip opening hood	2.87	4.1	1.18	3.2
Two seam opening hood	0.04	0.73	1.03	1.16

Table 8. The maximum principal stress of different monitor cross-section at the waist of the hood structure.

4. Conclusion

The chapter discussed several types of hood structures' safety and dynamic response under Wolong seismic wave, the acceleration peak of which was 0.6 m/s^2, using finite element method. The analysis results showed that:

1. Under seismic load, the peak value of maximum principal stress may exceed the tensile strength of structure material (C35). No matter setting opening or not, the seismic load can result in damage to the hood structure.
2. Differences of setting opening position can affect the peak value of maximum principal stress.
3. Although there is some variation because of the differences in types of hood, the stress maximum region is almost same, near to the waist of the hood structure.
4. Except the two seam opening hood, in the hood axial direction, the peak value of max principal stress appeared at the section II-II, which is 7 m to the hood and tunnel cross point.
5. Among these hoods, the peak of maximum principal stress value on two seam opening hood is the lowest. So this hood structure is recommended in tunnel entrance for high-speed railway line.

Acknowledgment

This chapter is supported by the National High Technology Research and Development Program ("863" Program) of China (grant No. 2011AA11A103-3-3-2).

Author details

Wang Ying-xue*, He Jun, Jian Ming, Chang Qiao-lei and Ren Wen-qiang

*Address all correspondence to: wangyingxue@home.swjtu.edu.cn

Key Laboratory of Transportation Tunnel Engineering, Ministry of Education, Southwest Jiaotong University, Chengdu, China

References

G. Cui. The seismic design calculation method and test study of tunnel shallow-buried portal and rupture stick-slipping section, Southwest Jiaotong University Doctor Degree Dissertation, 2010.

B. Gao, Z. Wang, S. Yuan, Y. Shen. Lessons learnt from damage of highway tunnels in Wenchuan earthquake, Journal of Southwest Jiaotong University, Vol. 44, No. 3, pp. 336–341, 2009.

Q. Jiang, Two-stage aerodynamic characteristics and parameter analysis of buffer structure at high-speed railway tunnel entrance, Southwest Jiaotong University Master Degree Dissertation, 2014.

Z. Wang, Z. Zhang, B. Gao, Y. Shen. Factors of seismic damage and fuzzy synthetic evaluation on seismic risk of mountain tunnel portals, Journal of Central South University (Science and Technology), Vol. 43, No. 3, pp. 1122–1130, 2012.

Z. Zheng. Analysis of mountain tunnel seismic damage study on dynamic response of tunnel entrance, Southwest Jiaotong University Master Degree Dissertation, 2007.

IntechOpen